International Journal of Mechanical, Industrial and Aerospace Sciences
ISSN: 2517-9950
Vol:11, No:5, 2017

Parametric and Analysis Study of the Melting in Slabs Heated by a Laminar Heat Transfer Fluid in Downward and Upward Flows

Radouane Elbahjaoui, Hamid El Qarnia

***Abstract*—**The present work aims to investigate numerically the thermal and flow characteristics of a rectangular latent heat storage unit (LHSU) during the melting process of a phase change material (PCM). The LHSU consists of a number of vertical and identical plates of PCM separated by rectangular channels. The melting process is initiated when the LHSU is heated by a heat transfer fluid (HTF: water) flowing in channels in a downward or upward direction. The proposed study is motivated by the need to optimize the thermal performance of the LHSU by accelerating the charging process. A mathematical model is developed and a fixed-grid enthalpy formulation is adopted for modeling the melting process coupling with convection-conduction heat transfer. The finite volume method was used for discretization. The obtained numerical results are compared with experimental, analytical and numerical ones found in the literature and reasonable agreement is obtained. Thereafter, the numerical investigations were carried out to highlight the effects of the HTF flow direction and the aspect ratio of the PCM slabs on the heat transfer characteristics and thermal performance enhancement of the LHSU.

***Keywords*—**Phase change material, thermal energy storage, latent heat storage unit, melting.

I. Introduction

DUE to the gap between thermal energy production and utilization, latent heat storage systems (LHSS) have become attractive thermal systems to conserving the available energy. These systems integrate PCMs which are characterized by relatively high energy storage density (compared with materials storing energy by sensible form) and small swing temperature during the phase transition. These two characteristics are advantageous for latent heat storage applications due to their advantage to reduce the volume of the storing materials without appreciable variation of the temperature around the melting temperature. LHSS were the subject of numerous research works during the last 20 years. This is due to the fact that they are used in several practical applications including solar building systems [1], [2], solar water heating systems [3], [4] and solar energy generation systems [5]-[9].

Charvát et al. [10] reported the experimental and numerical investigation of a heat storage unit containing 100 aluminum panels filled with PCM and 20 mm air gap (air channel) between the panels. A 1D mathematical model was developed and used for a parametric study. Mosaffa et al. [11] numerically studied the performance enhancement of a thermal energy storage (TES) unit employing multiple PCMs and using the effective heat capacity method. The storage unit is composed of a number of horizontal PCMs slabs separated by rectangular channels through which a HTF flows. The effects of the slab length, the thickness and the HTF channel gap on the storage performance were investigated using an energy based optimization. The results show that the optimum length is 1.3 m, the slab thickness is 10 mm and the air channel gap is 3.2 mm. The results also show that the system which can ensure comfort conditions has approximately a COP of 7.0 in the climate of Tabriz (Iran). Bechiri and Mansouri [12] analytically investigated the thermal performance of a LHSU composed of various PCM flat slabs heated by HTF flowing under laminar forced convection. The results show that the obtained exact solution gives a good estimation of the thermal behavior of the LHSU during charging and discharging processes. Lopez et al. [13] developed a numerical model taking into account conduction in the PCM plates and heat transfer between the airflow and the plates for TES in buildings. Halawa and Saman [14] carried out a numerical study of an air LHSU used for space heating. The LHSU consists of one dimensional rectangular ducts filled with PCM where the HTF flows between the PCM slabs. The effects of design parameters such as air mass flow, air gaps, slab dimension and charge/discharge temperatures differences on the heat transfer rate and air outlet temperature has been investigated. Ye et al. [15] numerically studied the melting of PCM not completely filled inside the cavities on heat transfer and fluid flow behaviors in a LHSU. They investigated the time of complete storage, volume expansion ratio, liquid fraction, heat flux, as well as velocity and temperature fields for a range of cavity volume fractions of PCM ranged from 35% and 95%. Computational results indicate that the time for complete energy storage increases with the increase of PCM cavity volume fraction, whereas, the volume expansion ratio decreases. Gharebaghi and Sezai [16] performed a numerical study of the thermal performance of a LHSU composed of slabs containing paraffin as PCM and metal fins where a HTF (air) flows in the gap between the PCM modules. The results show that the heat transfer rate to PCM can be enhanced by adding fins. Borderon et al. [17] modeled a storage system integrated in the ventilation circuit and composed of horizontal PCM sheets placed in a box beam

H. El Qarnia and R. Elbahjaoui are with Cadi Ayyad University, Faculty of Science Semlalia, Department of Physics, Fluid Mechanics and Energetic Laboratory, Marrakesh, B.P. 2390, Morocco (phone: +212)0666350016; e-mail: elqarnia@uca.ac.ma).

where air blows between the sheets and exchanges heat by convection with PCM. Lazaro et al. [18] experimentally studied a phase change thermal storage (PCTS) used for free-cooling. In this application, PCM is solidified during the night and then during the day, the inside air of a building can became cold by exchanging heat with PCM. El Qarnia [19] numerically studied the transient behavior of a latent heat thermal energy storage (LHTES) system composed of a number of PCM slabs separated by rectangular channels where a HTF flows and exchanges heat by forced convection with PCM. The effects of the control parameters on the thermal behavior of the LHTES are investigated. Ait Adine and El Qarnia [20] numerically studied the thermal performance of a LHSU using various PCMs. They conducted several numerical simulations in order to study the effects of the operating and geometric parameters. Elbahjaoui and El Qarnia [21] investigated the melting of PCM (Paraffin wax) dispersed with high conductive nanoparticles (alumina) filled inside rectangular plates heated by a laminar HTF (water) flow. The impacts of varying the volumetric fraction of nanoparticles, aspect ratio of plates, Reynolds number and Rayleigh number on the melting time, latent and sensible storage efficiencies were numerically evaluated. Wang et al. [22] numerically studied the heat charging and discharging performance of a shell-and-tube LHSU used n-octadecane as a PCM. They evaluated the impact of the inlet temperature and mass flow rate of the HTF on the melting and solidification processes characteristics. Elbahjaoui and El Qarnia [23] numerically studied the storage performance of a shell-and-tube thermal storage system heated by a laminar pulsed HTF flow during the charging process. The effects of the pulsating frequency, the pulsating amplitude, the Reynolds number and the Stefan number on the thermal performance of the storage system were numerically investigated. The results reveal that the use of a pulsed HTF flow instead of a stationary flow enhances the melting rate of PCM for high pulsating amplitude and less pulsating frequency (less than 0.052).

In most of the rectangular LHSS mentioned above, PCM plates are placed horizontally. In addition, the effect of natural convection is not taken into account and can be neglected as reported by Laouadi and Lacroix [24]. The proposed work overcomes this limitation by taking into consideration the effect of natural convection during the melting of a PCM (P116) placed in vertical slabs composing a LHSU. Because the melting process is initiated by circulating a HTF (water) between the PCM plates, the effect of the flow direction (downward and upward flow) is also taken into account.

II. Mathematical Model

A. Problem Statement

A schematic of the LHSU studied in this work is shown in Fig. 1 (a). It consists of (N+1) several vertical PCM slabs separated by N rectangular channels through which a HTF flows. A representative volume in the LHSU, which is repetitive, is chosen. The solution domain is shown in Fig. 1 (b). It consists of a PCM rectangular enclosure of width, d/2, and height, H, and a HTF channel of width, w/2, and height, H. The PCM and HTF used are, respectively, paraffin wax P116 and water. At time, t = 0, the PCM is solid at its melting temperature, Tm. The melting process of the PCM is initiated, at t > 0, when HTF (hot water) flows into channels. The phage change process continues until all the PCM was completely melted which corresponds to full charge of the LHSU.

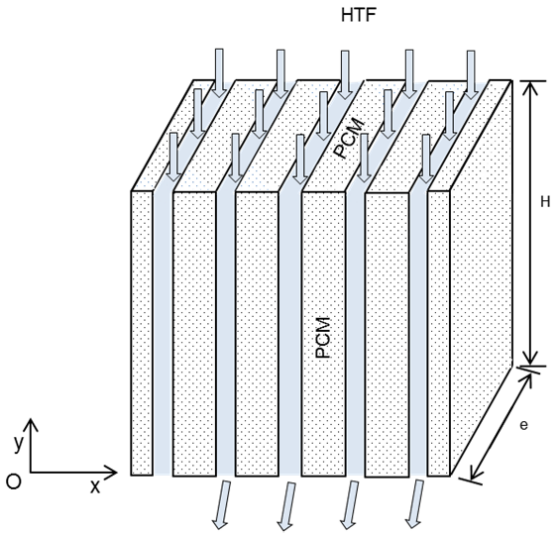

Fig. 1 (a) LHSU

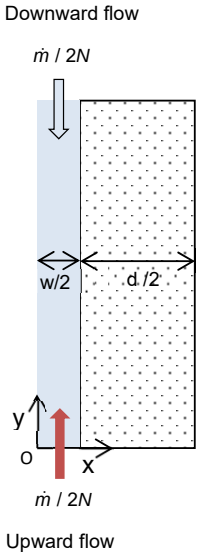

Fig. 1 (b) Computational domain

B. Assumptions

In order to model heat transfer by natural convection and conduction in the PCM and by forced convection in the HTF flow, some assumptions are adopted. It is assumed that the transient heat transfer and fluid flow are 2D. The PCM is assumed to be pure, homogeneous, and isotropic. Thermo-physical properties of HTF and PCM are assumed to be constant in the temperature range considered in this study (47-

60 °C). Thermo-physical properties of PCM are the same in both phases, except the thermal conductivity which varies according to the PCM phase. The PCM liquid phase and HTF are Newtonian and incompressible. The HTF and liquid PCM flows are assumed laminar. The HTF flow is assumed dynamically developed. The Boussinesq approximation is valid for the PCM liquid phase density variations in the buoyancy source term. Viscous dissipation is neglected. The wall separating the HTF and PCM is assumed to be very thin, so its thermal resistance is neglected. The contact between the PCM and the wall is perfect and permanent. The solid PCM is immobilized. The reference temperature, $T_{ref} = T_{melt}$, and the reference density, $\rho_{ref} = \rho\ (T = T_{melt})$, are made to the melting point.

C. Governing Equations and Numerical Procedure

In this work, the enthalpy-based method was used to simulate the melting process of PCM. In this method, the solid-liquid interface and the two phases are modeled as a porous medium. Based on the previous simplifying assumptions, the unsteady two dimensional governing equations for conservation of mass, momentum and energy are written as follows:

Continuity equation:

$$\frac{\partial(\rho_m u_m)}{\partial x}+\frac{\partial(\rho_m v_m)}{\partial y}=0 \tag{1}$$

Momentum equations:

$$\frac{\partial(\rho_m u_m)}{\partial t}+\frac{\partial(\rho_m u_m u_m)}{\partial x}+\frac{\partial(\rho_m v_m u_m)}{\partial y}=-\frac{\partial p}{\partial x}+\frac{\partial}{\partial x}(\mu_m\frac{\partial u_m}{\partial x})+\frac{\partial}{\partial y}(\mu_m\frac{\partial u_m}{\partial y})+S_u \tag{2a}$$

$$\frac{\partial(\rho_m v_m)}{\partial t}+\frac{\partial(\rho_m u_m v_m)}{\partial x}+\frac{\partial(\rho_m v_m v_m)}{\partial y}=-\frac{\partial p}{\partial y}+\frac{\partial}{\partial x}(\mu_m\frac{\partial v_m}{\partial x})+\frac{\partial}{\partial y}(\mu_m\frac{\partial v_m}{\partial y})+S_v \tag{2b}$$

Energy equations:

For PCM

$$\frac{\partial(\rho_m h)}{\partial t}+\frac{\partial(\rho_m u_m h)}{\partial x}+\frac{\partial(\rho_m v_m h)}{\partial y}=\frac{\partial}{\partial x}(\frac{k_m}{c_m}\frac{\partial h}{\partial x})+\frac{\partial}{\partial y}(\frac{k_m}{c_m}\frac{\partial h}{\partial y})+S_h \tag{3}$$

For HTF (in downward flow)

$$\frac{\partial T_f}{\partial t}+\frac{\partial(v_f T_f)}{\partial y}=\frac{\partial}{\partial x}(\alpha_f\frac{\partial T_f}{\partial x})+\frac{\partial}{\partial y}(\alpha_f\frac{\partial T_f}{\partial y}) \tag{4}$$

where vf in (4) is the velocity component of Poiseuille flow in plane channel. It is given by:

$$v_f=\frac{3}{2}V_m(1-(\frac{x}{w/2})^2) \tag{5}$$

The source terms in the momentum equations are as:

$$S_u=-C\frac{(1-f)^2}{(f^3+b)}u_m \tag{6a}$$

$$S_v=-C\frac{(1-f)^2}{(f^3+b)}v_m+\rho_m g\beta(T_m-T_{melt}) \tag{6b}$$

The source term in the PCM energy equation is written as:

$$S_h=-\rho_m\Delta H_m\frac{\partial f}{\partial t} \tag{6c}$$

The specific enthalpy is given by:

$$h=\int_{T_{melt}}^{T}c_m\,dT_m+h(T_{melt})\quad(h(T_{melt})=0) \tag{6d}$$

D. Boundary and Initial Conditions

The initial and boundary conditions for the conservation equations are as:

$$t=0\quad T_m=T_f=T_{melt},\ u_m=v_m=0 \tag{7a}$$

$$x=0\quad \frac{\partial T_f}{\partial x}=0 \tag{7b}$$

$$y=0\quad \frac{\partial T_m}{\partial y}=\frac{\partial T_f}{\partial y}=0,\ u_m=v_m=0 \tag{7c}$$

$$x=w/2\quad k_m\frac{\partial T_m}{\partial x}=k_f\frac{\partial T_f}{\partial x},\ u_m=v_m=0 \tag{7d}$$

$$x=w/2+d/2\quad \frac{\partial T_m}{\partial y}=0,\ u_m=0,\frac{\partial v_m}{\partial x}=0 \tag{7e}$$

$$y=H\quad \frac{\partial T_m}{\partial y}=0, T_f=T_{f,in},\ u_m=v_m=0 \tag{7f}$$

Because the mass of PCM is kept constant, in this study, the width, w, and the height, H, of the PCM enclosure can be expressed as follows:

$$H=\sqrt{\frac{AM}{2\rho_m N e}} \tag{8a}$$

$$d=\sqrt{\frac{2M}{\rho_m NA e}} \tag{8b}$$

where A is the aspect ratio of the enclosure, H/(d/2).

The melting of PCM is simulated using the enthalpy fixed-grid method [25]. In this method, the solid-liquid interface between the solid and melt is handled implicitly with the two phase regions modeled as a porous medium. The liquid

fraction varies smoothly across this porous, so-called mushy zone (also interface region). This latter is modeled via the phase fractions, which are incorporated in the source terms in the governing equations to account for the phase change process.

The transport equations are integrated over each control volume in the (x, y) plane using the finite volume approach developed by [26].

For the temporal discretization, the first-order and fully implicit backward Euler method is used. The Tree-Diagonal Matrix Algorithm (TDMA) is used for solving the algebraic equations. The iterative solution continues until convergence of the flow and temperature fields at each time step. Solution was declared converged when the largest local relative change in the HTF temperature is less than 10^{-6} and when the largest mass and thermal balances, for the PCM enclosure, were less than 10^{-8} and $5x10^{-3}$, respectively.

III. Detailed Study

This section focuses on the effects of the HTF flow direction (upward or downward direction) and the aspect ratio of the PCM enclosure on the flow and thermal characteristics of the LHSU during the melting process of the PCM. The aspect ratio, A, ranges from 0.5 to 16., the number of the HTF channels, N , varies between 10 and 60 and the mass flow rate, $\dot{m}$, ranges from 0.05 kg/s to 0.6 kg/s. The values of the other governing parameters are fixed at their reference values as follows: M = 80 kg, e = 1 m, w = 6 mm and T_{fi} = 60°C. The number of the HTF channels, N , and the mass flow rate, $\dot{m}$, are kept constant at values 10 and 0.1 kg/s, respectively. It should be noted that the height, H, and width, d, of the PCM enclosure have been calculated from (8a) and (8b).

A. Effects of the HTF Flow Direction on Streamlines and Isotherms

Fig. 2 shows the streamlines describing the flow field in the liquid PCM for the case of HTF downward flow at times: 35 min, 75 min, 110 min and 195 min. The case of an HTF upward flow is also investigated and illustrated in Fig. 3, for comparison. The aspect ratio, the number of rectangular channels and the mass flow rate are equal to 6, 10 and 0.1 kg/s, respectively. These figures show that a part of heat is transmitted to the PCM and thereby causes its melting startup for both cases, upward and downward flow of HTF. At the same time, natural convection begins to develop near the heated wall. The liquid PCM flow is in the clockwise direction, upward close to the heated wall and downward near the melting front. As can be seen in Figs. 2 (a) and (b), the flow is mono-cellular where a single cell is formed in the melted portion. The heated liquid moves to the top part of the PCM slab before impinging on the melting front. The displacement of the hot liquid PCM upwardly of the slab causes an accelerated melting in this region. This causes deformation and rapid progression of the melting front in this section of PCM slab. Compared to the case of upward flow, the melt front is deformed more quickly in the upper part of the PCM slab for the case of a downward flow (t = 35min, 75 and 110 min). As time progresses, the liquid volume widens, and the effect of natural convection intensifies. At t = 110 min, the liquid PCM flow remains mono-cellular for a HTF downward flow while for the case of an upward flow of HTF, it becomes bi-cellular. As heating ongoing (t = 195 min), the liquid PCM region is more extended, and the cells are combined together for the case of HTF upward flow with appearance of a new counter-clockwise cell in the lower right corner of PCM slab. In the case of HTF downward flow, at t =195 min, in addition to the appearance of a new anti-clockwise cell in the right corner, the clockwise cell is divided into a cellule located in the upper part and another that has moved into the bottom part of the slab.

Fig. 4 shows the temperature contours in the PCM slabs, for the case of HTF downward flow, at the same aforementioned times: 35 min, 75 min, 110 min and 195 min. The case of HTF upward flow is also treated as illustrated in Fig. 5. The same aforementioned values of the aspect ratio, the number of HTF channels and the mass flow rate are considered. Figs. 4 and 5 show that, for both cases of HTF flow direction (upward or downward flow), the melted PCM close to the heated wall moves towards the top region of the enclosure as melting progresses. Such a movement is due to natural convection occurring inside the melted PCM. As a consequence, a non-uniform temperature distribution occurs in the vertical direction. It should be noted that, for both cases of HTF flow direction, the highest temperature takes place in the **-op region of the PCM enclosure. One can also note that the maximum temperature is achieved in the case of a downward flow of HTF.

B. Effects of the Aspect Ratio of PCM Slabs

To compare the thermal behavior and performance of the LHSU heated by a downward and an upward HTF flow, two different storage efficiencies were defined. The first efficiency, called the sensible storage efficiency, is associated to the storage of energy by sensible heat. It is defined as the ratio between the sensible energy stored in the PCM and the maximum energy that can be stored in PCM. It is given as:

$$\varepsilon_{sen} = \frac{\int_{x=w/2}^{w/2+d/2}\int_{y=0}^{H} 2N\rho_m c_m (T_m - T_{melt})dx\,dy}{M\Delta H + M c_m (T_{f,in} - T_{melt})} \quad (9)$$

The second efficiency, called the latent storage efficiency, concerns the storage of energy by latent heat. It is defined as the ratio between the stored energy by latent heat and the maximum energy that can be stored in PCM. It is expressed as:

$$\varepsilon_{lat} = \frac{f\,M\Delta H}{M\Delta H + M c_m (T_{f,in} - T_{melt})} \quad (10)$$

The latent storage efficiency, ε_{lat} , achieves its maximum value when the PCM is completely melted (f = 1). This

maximum value, as can be concluded from the latest expression, is lower than the value 1. The sensible storage efficiency, ε_{sen}, reaches its maximum value when the thermal equilibrium is established between PCM and HTF. At this moment, the PCM is heated to the HTF inlet temperature and the sum of the two storage efficiencies becomes equal to 1 ($\varepsilon_{sen} + \varepsilon_{lat} = 1$).

The effect of the PCM enclosure aspect ratio, A, on the time wise variation of the sensible storage efficiency, ε_{sen}, is illustrated in Fig. 6, for both cases, HTF downward and upward flows. As can be seen in this figure, the sensible storage efficiency increases because to the increase of the mean PCM temperature. Its time evolution is characterized by two stages. During the first stage, the PCM undergoes phase change process. It stores energy mainly by latent heat which explains the relatively lower change of the sensible energy storage with time. During the second stage, when the melting has completed, the sensible energy storage increases rapidly compared to its variation during the first stage due to the rapid increase of the mean temperature of the PCM. Indeed, during such a stage, the PCM which is completely liquid, stores energy mainly by sensible heat and its mean temperature rises rapidly. The sensible storage efficiency achieves its maximum value of 0.126 and remains constant thereafter. This maximum value is achieved when the charging of the LHSU is completed. This means that the temperature of the PCM has become equal to the HTF inlet temperature and the thermal equilibrium has been established. The time required for complete charge of the LHSU for HTF downward flow case is 587.8 min, 332.6 min and 161.4 min for A = 0.5, 2 and 16, respectively. For HTF upward flow case, this time is 653.4 min, 386.7 min and 209.17 min for A = 0.5, 2 and 16, respectively. Based on these results, it can be noted that for both cases of HTF flow direction, the maximum sensible heat is early stored in PCM slabs for a higher aspect ratio. This behavior is justified by the fact that the increase of the aspect ratio leads to an increase of the heat exchange surface between the HTF and PCM. One can also conclude that compared to the upward flow case, the downward flow case insures a quick charge of the LHSU when the aspect ratio, A, ranges from 0.5 to 16.

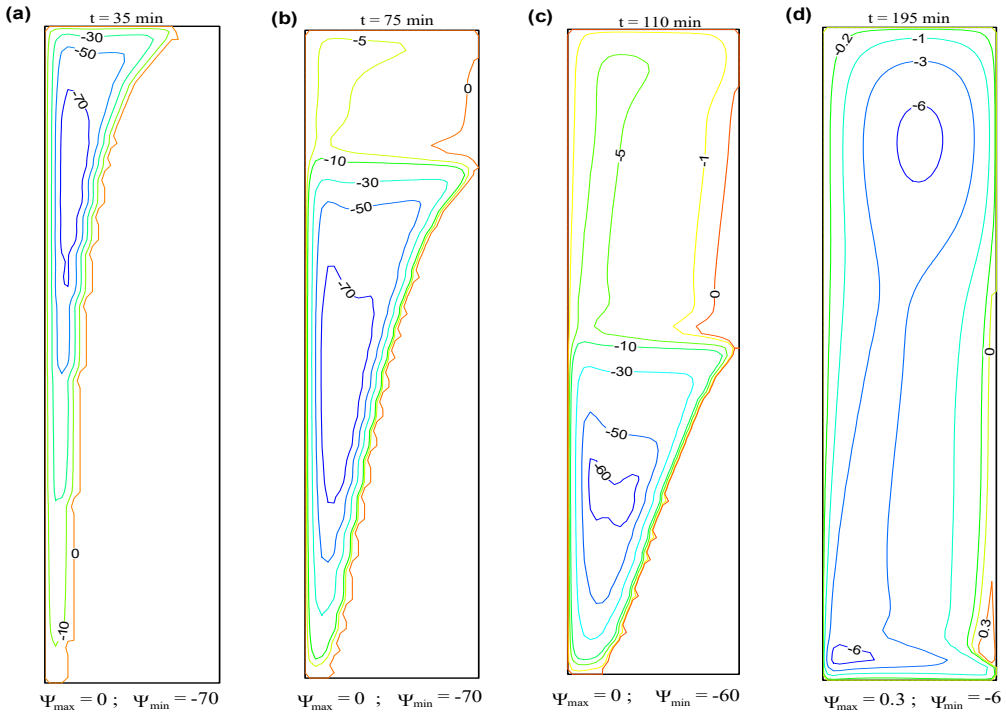

Fig. 2 Streamlines for a downward HTF flow in channels at (a) t = 35min, (b) 75 min, (c) 110 min and (d) 195 min for A = 6

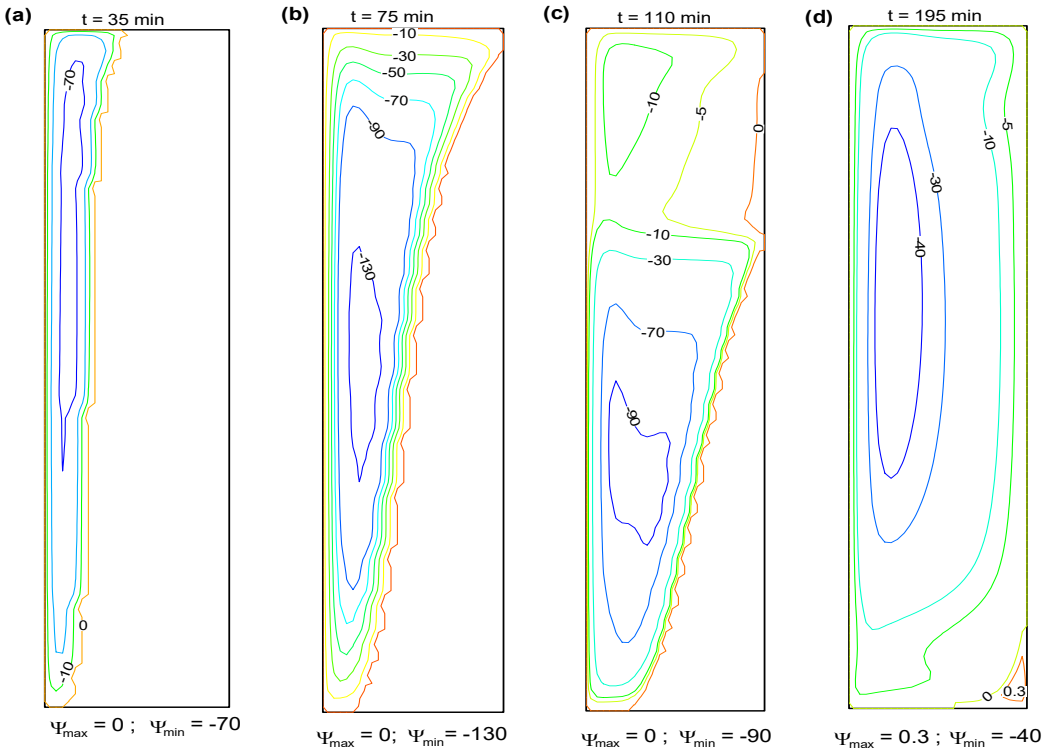

Fig. 3 Streamlines for an upward HTF flow in channels at (a) t = 35min, (b) 75 min, (c) 110 min and (d) 195 min for A = 6

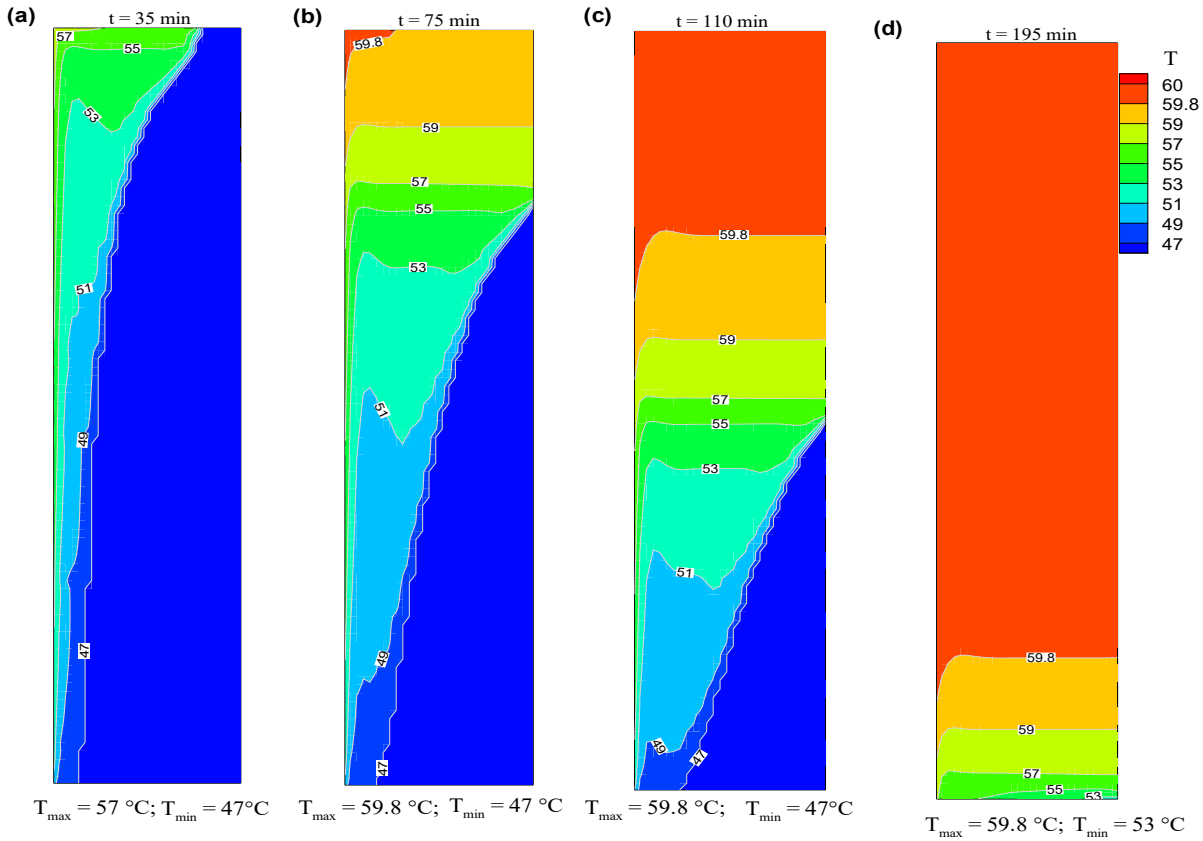

Fig. 4 Isotherms for a downward HTF flow in channels at (a) t = 35min, (b) 75 min, (c) 110 min and (d) 195 min for A = 6

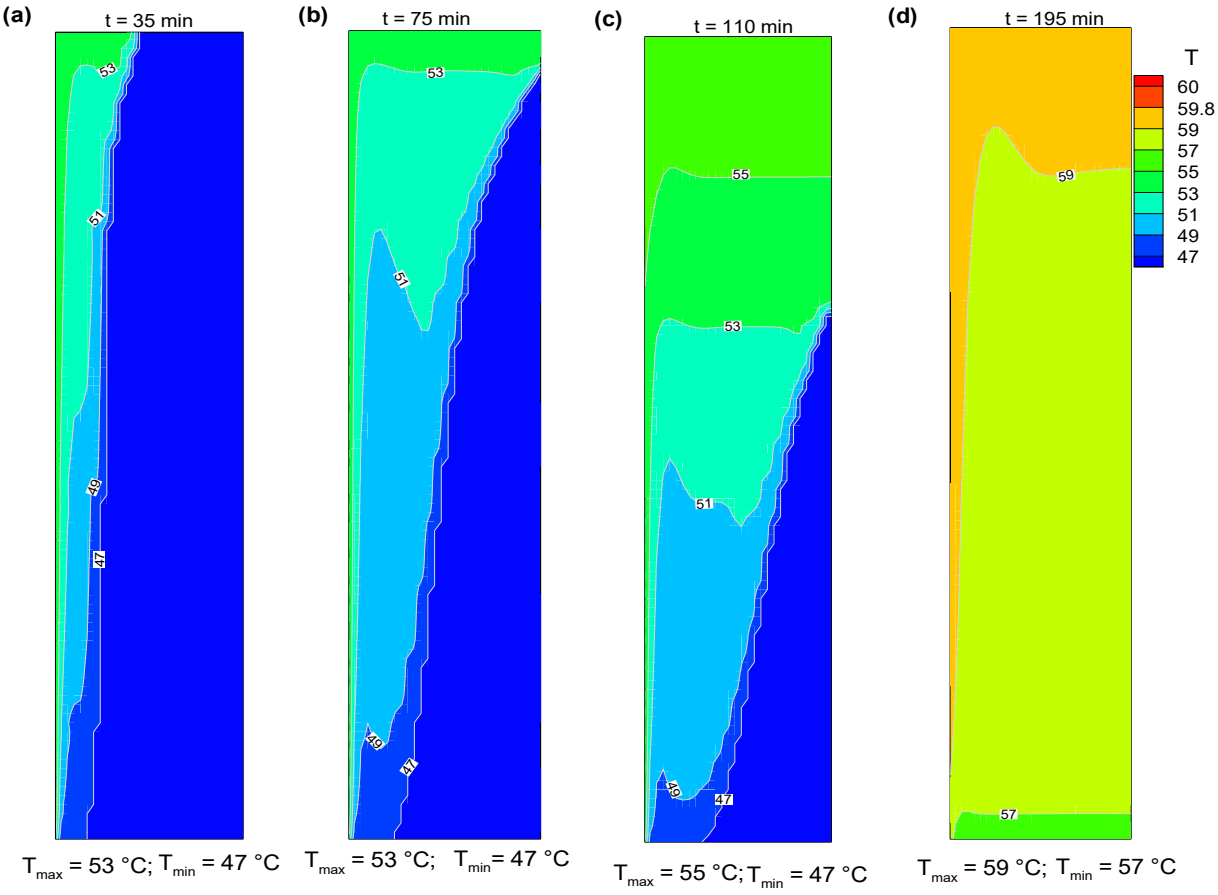

Fig. 5 Isotherms for an upward HTF flow in channels at (a) t = 35min, (b) 75 min, (c) 110 min and (d) 195 min for A = 6

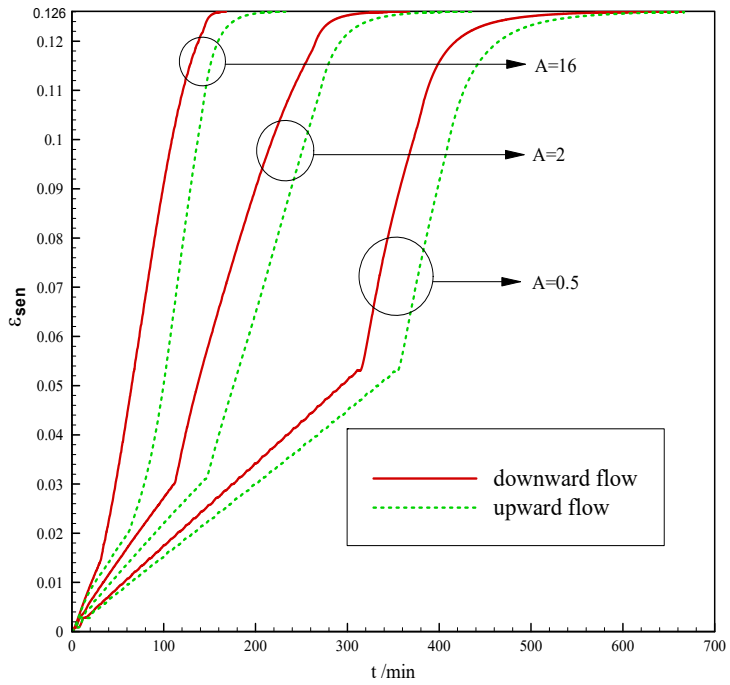

Fig. 6 Effect of the aspect ratio, A, on the time wise variation of the sensible storage efficiency for a downward and an upward HTF flows

The effect of the aspect ratio, A, on the time wise variation of the latent storage efficiency, ε_{lat}, is illustrated in Fig. 7, for both cases of HTF flow direction. As can be seen in this figure, the latent storage efficiency increases nonlinearly to reach its maximum value of 0.874 and then remains constant. This maximum value is reached when the PCM is fully melted. The melting time for the case of HTF downward flow direction is 379.6 min, 264 min and 144.4 min for A = 0.5, 2 and 16, respectively. In the case of a HTF upward flow direction, the melting time is 409 min, 271.16 min and 143.83 min for A = 0.5, 2 and 16, respectively. It should be noted that for both cases of flow direction, the melting time is reduced with the increase of the aspect ratio. This is due to the enhancement of heat transfer caused by the increase of the heat exchange surface. Fig. 7 also shows that the difference between the melting times of PCM associated to upward and downward flows decreases with the increase of the aspect ratio, A. For A = 16, this melting time difference is negative which means that the upward flow direction becomes more favorable for the melting process.

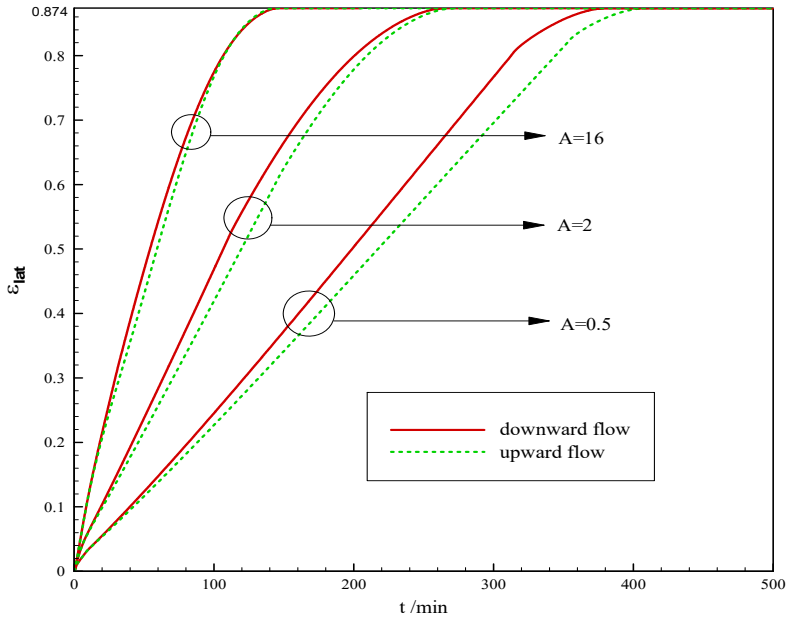

Fig. 7 Effect of the aspect ratio, A, on the time wise variation of the latent storage efficiency for a downward and an upward HTF flows

IV. Conclusion

In the present study, a numerical analysis of the melting of a PCM (Paraffin wax P116) in a rectangular thermal storage unit heated by a downward and an upward flow of HTF (water) was conducted. So, a mathematical model based on the conservation equations of mass, momentum and energy has been developed to investigate the effect of the HTF flow direction and the aspect ratio of the PCM slabs on the thermal performance of the storage unit. The results show that the increase in the aspect ratio of PCM slabs reduces significantly the melting time. The results also reveals that for a PCM slab aspect ratio, the circulation of HTF in the upward direction is more favorable for melting the PCM.

References

[1] F. Kuznik, J. Virgone, "Experimental assessment of a phase change material for wall building use," Applied Energy, (2009), pp. 2038-2046.
[2] W. Xiao, X. Wang, Y. Zhang, "Analytical optimization of interior PCM for energy storage in a lightweight passive solar room," Applied Energy, (2009), pp. 2013-2018.
[3] C. Garnier, J. Currie, T. Muneer, "Integrated collector storage solar water heater: Temperature stratification," Applied Energy, (2009), pp. 1465-1469.
[4] K. Sutthivirode, P. Namprakai, N. Roonprasang, "A new version of a solar water heating system coupled with a solar water pump," Applied Energy, (2009), pp. 1423-1430.
[5] Z.D. Cheng, Y.L. He, J. Xiao, Y.B. Tao, R.J. Xu, "Three-dimensional numerical study of heat transfer characteristics in the receiver tube of parabolic trough solar collector," International Communications in Heat and Mass Transfer, (2010), pp. 782-787.
[6] D. Brosseau, J.W. Kelton, D. Ray, M. Edgar, "Testing of Thermocline Filler Materials and Molten-Salt Heat Transfer Fluids for Thermal Energy Storage Systems in Parabolic Trough Power Plants," J. Sol. Energy Eng., (2005), pp. 8.
[7] Y.-L. He, J. Xiao, Z.-D. Cheng, Y.-B. Tao, "A MCRT and FVM coupled simulation method for energy conversion process in parabolic trough solar collector," Renewable Energy, (2011), pp. 976-985.
[8] Y.B. Tao, Y.L. He, "Numerical study on coupled fluid flow and heat transfer process in parabolic trough solar collector tube," Solar Energy, (2010), pp. 1863-1872.
[9] Z. Yang, S.V. Garimella, "Molten-salt thermal energy storage in thermoclines under different environmental boundary conditions," Applied Energy, (2010), pp. 3322-3329.
[10] P. Charvát, L. Klimeš, M. Ostrý, "Numerical and experimental investigation of a PCM-based thermal storage unit for solar air systems," Energy and Buildings, (2014), pp. 488-497.
[11] A.H. Mosaffa, C.A. Infante Ferreira, F. Talati, M.A. Rosen, "Thermal performance of a multiple PCM thermal storage unit for free cooling," Energy Conversion and Management, (2013), pp. 1-7.
[12] M. Bechiri, K. Mansouri, "Exact solution of thermal energy storage system using PCM flat slabs configuration," Energy Conversion and Management, (2013), pp. 588-598.
[13] J. P. A. Lopez, F. Kuznik, D. Baillis, J. Virgone, "Numerical modeling and experimental validation of a PCM to air heat exchanger," Energy

and Buildings, (2013), pp. 415-422.
[14] E. Halawa, W. Saman, "Thermal performance analysis of a phase change thermal storage unit for space heating," Renewable Energy, (2011), pp. 259-264.
[15] W.-B. Ye, D.-S. Zhu, N. Wang, "Fluid flow and heat transfer in a latent thermal energy unit with different phase change material (PCM) cavity volume fractions," Applied Thermal Engineering, (2012), pp. 49-57.
[16] M. Gharebaghi, I. Sezai, "Enhancement of heat transfer in latent heat storage modules with internal fins," Numerical Heat Transfer, Part A: Applications, (2007), pp. 749-765.
[17] J. Borderon, J. Virgone, R. Cantin, "Modeling and simulation of a phase change material system for improving summer comfort in domestic residence," Applied Energy, (2015), pp. 288-296.
[18] A. Lazaro, P. Dolado, J.M. Marín, B. Zalba, "PCM–air heat exchangers for free-cooling applications in buildings: Experimental results of two real-scale prototypes," Energy Conversion and Management, (2009), pp. 439-443.
[19] H. El Qarnia, "Theoretical study of transient response of a rectangular latent heat thermal energy storage system with conjugate forced convection," Energy Conversion and Management, (2004), pp. 1537-1551.
[20] H. Ait Adine, H. El Qarnia, "Numerical analysis of the thermal behaviour of a shell-and-tube heat storage unit using phase change materials," Applied Mathematical Modelling, (2009), pp. 2132-2144.
[21] R. Elbahjaoui, H. El Qarnia, "Transient behavior analysis of the melting of nanoparticle-enhanced phase change material inside a rectangular latent heat storage unit," Applied Thermal Engineering, (2017), pp. 720-738.
[22] W.-W. Wang, K. Zhang, L.-B. Wang, Y.-L. He, "Numerical study of the heat charging and discharging characteristics of a shell-and-tube phase change heat storage unit," Applied Thermal Engineering, (2013), pp. 542-553.
[23] R. Elbahjaoui, H. El Qarnia, "Numerical Study of a Shell-and-Tube Latent Thermal Energy Storage Unit Heated by Laminar Pulsed Fluid Flow" Heat Transfer Engineering, (2016).
[24] A. Laouadi, M. Lacroix, "Thermal performance of a latent heat energy storage ventilated panel for electric load management," International Journal of Heat and Mass Transfer, (1999), pp. 275-286.
[25] K.-G. Kang, H.-S. Ryou, "Computation of solidification and melting using the PISO algorithm," Numerical Heat Transfer, Part B: Fundamentals, (2004), pp. 179-194.
[26] S.V. Patankar, Numerical Heat Transfer and Fluid Flow, Hemisphere Publishing Corporation, New York, 1980.